ice | science

**ICE**
Institution of Civil Engineers

publishing

# Biomineralised interpenetrating network hydrogels for bone tissue engineering

[1] **Ganesh Ingavle** PhD
Postdoctoral Research Fellow, Biomaterials and Medical Devices Research Group, School of Pharmacy and Biomolecular Sciences, University of Brighton, Brighton, UK

[2] **Venkata Avadhanam** MS, FRCS, FRCOphth
Surgeon, Sussex Eye Hospital, Brighton and Sussex Medical School, Brighton, UK

[3] **Yishan Zheng** PhD
Postdoctoral Research Fellow, Biomaterials and Medical Devices Research Group, School of Pharmacy and Biomolecular Sciences, University of Brighton, Brighton, UK

[4] **Christopher Liu** MD, FRCOphth
Professor and surgeon, Sussex Eye Hospital, Brighton and Sussex Medical School, Brighton, UK

[5] **Susan Sandeman** PhD*
Reader and Principal Research Fellow, Biomaterials and Medical Devices Research Group, School of Pharmacy and Biomolecular Sciences, University of Brighton, Brighton, UK

Hydrogels are attractive for tissue engineering applications due to their incredible versatility, but their use is limited by inadequate mechanical strength and poor biocompatibility. In this study, to better mimic the mineral component and the mechanical strength of natural bone, two biocompatible materials, 2-hydroxyethyl agarose and poly (ethylene glycol) diacrylate, were combined with nanocrystalline hydroxyapatite (nHAp)-coated poly(lactic-co-glycolic acid) (PLGA) microspheres. A novel composite interpenetrating network (IPN) hydrogel scaffold was created to investigate its mechanical and osteoconductive performance for bone tissue engineering-related applications. The inclusion of nHAp-coated PLGA microspheres in an IPN hydrogel led to an increase in compressive modulus. In the absence of nHAp-coated microspheres, cell viability dropped to 59·1% at 3 weeks post-encapsulation. However, by incorporating nHAp-coated microspheres, cell viability improved to 80·6%. The capacity of composite IPN hydrogels to promote bone formation in cell culture was assessed. In the presence of mineralised microspheres, a composite IPN gel showed a significant increase in alkaline phosphatase activity and calcium (Ca) deposition following 3 weeks of incubation when compared with plain IPNs. This technology may be also applied to other cell-based applications where the improved mechanical integrity and osteoconductivity of cell-containing IPN hydrogels may be used to mimic bone tissue replacement.

## 1. Introduction

Polymeric hydrogels hold great potential for bone tissue engineering, but their application is limited by the requirement for a hydroxyapatite (HAp)-rich micro-environment, poor cell affinity and mechanical properties, as well as by their limited ability to allow cell spreading of anchorage-dependent cells such as osteoblasts. Most synthetic hydrogels typically exhibit minimal biological activity,[1,2] with a lack of desired mechanical integrity, and may not provide an ideal environment for encapsulated cells. Mimicking the mechanical aspects and biological micro-environment of natural tissues can be used to enhance the functionality of engineered tissues, and the development of hydrogels that are stronger mechanically may be beneficial for various biomedical applications.[3,4] By generating composite hydrogels, it may be possible to reproduce the properties of a natural extracellular matrix (ECM). One approach to creating composite materials is the fabrication of an interpenetrating network (IPN) of polymers.

*Corresponding author e-mail address: s.sandeman@brighton.ac.uk

**Bioinspired, Biomimetic and Nanobiomaterials**
Volume 5 Issue BBN1

**Biomineralised interpenetrating network hydrogels for bone tissue engineering**
Ingavle, Avadhanam, Zheng, Liu and Sandeman

An IPN is a polymer comprising two or more networks that are at least partially interlaced on a polymer scale, but not covalently linked to each other. As the two networks are independent of each other while being physically interlocked, this type of network is termed an IPN. Several studies[5–10] discovered that for a variety of hydrogel IPNs and semi-IPNs, the mechanical performance of the IPNs was far superior to either of the 'parent' networks. They reported the synthesis of IPNs and semi-IPNs using various combinations of biological and synthetic polymers with substantially improved mechanical properties.[5–10] 2-Hydroxyethyl agarose and poly(ethylene glycol) (PEG) were selected as the materials to create a novel IPN scaffold based on their common use in tissue engineering studies and to approximate a combination of networks with asymmetric mechanical properties. A rigid, brittle network interpenetrated with a softer, more ductile network is theorised to serve as the key to enhanced mechanical performance in composite IPN gels. In addition, Ingavle et al.[11–14] recently applied 2-hydroxyethyl agarose-poly(ethylene glycol) diacrylate (PEG-DA) IPN hydrogels to cartilage tissue engineering and showed that it was possible to encapsulate viable cells and provide a significant improvement in mechanical performance relative to the two constituent hydrogels. Previous studies of 2-hydroxyethyl agarose/PEG-DA IPNs showed improvement in mechanical performance compared to both single networks, but it can be further improved by increasing the concentration of either first or second network and the molecular weight (MW) of PEG-DA while still maintaining cell performance.

Synthetic IPN hydrogels alone cannot provide an ideal environment to support cell adhesion and bone tissue formation due to their biologically inert nature. ECM mimetic modifications and the provision of a nanocrystalline hydroxyapatite (nHAp)-rich micro-environment within synthetic hydrogels materials may be used to modulate specific cellular responses.[15] However, the development of an IPN biomaterial with both biological and synthetic components and ECM-mimetic modifications remains a significant challenge. A range of bioactive, inorganic nanoparticles such as nHAp, calcium phosphate, bioactive glasses and silica consist of minerals that are already present in the body, are necessary for the normal functioning of human bone tissue and have shown favourable biological responses.[16] HAp is a mineral component of natural bone and exhibits osteoconductive properties, osteoinductive properties, bone-bonding abilities and slow degradation on site.[17] It has been well documented that synthetic nHAp can promote new bone ingrowth through osteoconductive mechanisms without causing any local or systemic toxicity, inflammation or a foreign body response.[18,19]

The production of IPN hydrogels with improved cell adhesion to enhance osteogenesis requires the use of materials with greater osteoconductivity to nucleate calcium, integrate with surrounding bone and promote bone formation. The osteoconductivity of biodegradable polymers such as poly(lactic-co-glycolic acid) (PLGA) can be successfully enhanced through substrate immersion in simulated body fluid (SBF) to create an external-environment carbonated apatite coating similar to that found on native bones.[20,21] Such coatings improve the osteoconductivity of the polymer, provide nucleation sites for cell secreted calcium and enhance the potential osseointegration with host tissue. Apatite-coated substrata including scaffolds and injectable microspheres have been examined by a number of investigators for their ability to contribute towards bone defect repair.[22–24] Recently, Davis et al.[25] examined the capacity of mineralised poly(lactide-co-glycolide) (PLG) microspheres suspended within fibrin hydrogels to enhance the osteoconductivity of fibrin gels. Pre-mineralised PLGA microspheres suspended in a fibrin gel achieved significant increases in bone mineral density over non-mineralised fibrin gel when implanted in a rodent calvarial defect over 12 weeks. Polymeric microspheres are less dense than bioceramics such as β-tricalcium phosphate or HAp, thus allowing for improved distribution throughout the gel and improved spatial interaction with osteogenic cells.

Although several studies have investigated the effect of bioactive nanoparticles on improved cell response and promotion of ECM synthesis in a single network hydrogel,[16,26–32] there have been no reports investigating the performance of osteoblasts in IPN hydrogels. In addition, to date, hybrids or composites of HAp with some traditional hydrogels have been developed.[33–36] However, the combination of cell-containing 2-hydroxyethyl agarose/PEG-DA IPN hydrogel with nHAp-coated PLGA microspheres and its impact on cell behaviour have not yet been reported. This study describes the development of a photo-cross-linked IPN hydrogel of 2-hydroxyethyl agarose and PEG-DA for application to bone tissue engineering. A photo-cross-linked 2-hydroxyethyl agarose/PEG-DA IPN hydrogel incorporating nHAp-coated PLGA microspheres was designed to provide improved mechanical strength as well as to promote cell spreading, proliferation and osteogenic differentiation. This study was innovative in two primary aspects: bringing IPN technology to bone tissue engineering and incorporating biomineralised microspheres as a bioactive signal to promote osteoconductivity in mechanically strong IPN scaffold. It is hypothesised that the inclusion of mineralised polymeric microspheres within IPN hydrogels would enhance viable cell growth and osteoconductivity and increase the osteogenic potential of this composite gel as well as stimulate bone formation in cell culture. A series of nHAp-coated PLGA microsphere-incorporated hydrogels based on an IPN of 2-hydroxyethyl agarose and PEG-DA were developed to optimise material properties and support for pre-osteoblast spreading and proliferation as well as osteogenic differentiation. The ratio of 2-hydroxyethyl agarose and PEG-DA was varied in order to fine-tune these properties. The pore structure, pore wall morphology, mechanical properties, long-term cell survival and the osteogenic response of human mesenchymal stem cells (hMSCs) to the improved composite IPN scaffolds were investigated in order to optimise these materials for bone-substitution applications.

**Bioinspired, Biomimetic and Nanobiomaterials**
Volume 5 Issue BBN1

**Biomineralised interpenetrating network
hydrogels for bone tissue engineering**
Ingavle, Avadhanam, Zheng, Liu and Sandeman

## 2. Experimental

### 2.1 Materials

2-Hydroxyethyl agarose, PEG-DA (MW 6000 Da) and photoinitiator 2,2-dimethoxy-2-phenylacetophenone (Irgacure 651), PLGA pellets with a copolymer ratio of 85:15 (lactic:glycolic DL (%)) and MWs of 50 000–70 000 were obtained from Sigma–Aldrich (Steinheim, Germany). Modified simulated body fluid (mSBF) was prepared as previously described[37] and consisted of the following reagents dissolved in distilled water ($H_2O$): 141 mM sodium chloride (NaCl), 5·0 mM calcium chloride ($CaCl_2$), 4·2 mM sodium bicarbonate ($NaHCO_3$), 4·0 mM potassium chloride (KCl), 2·0 mM monopotassium phosphate ($KH_2PO_4$), 1·0 mM magnesium chloride ($MgCl_2$) and 0·5 mM magnesium sulfate ($MgSO_4$). The solution was held at pH = 6·8 to avoid homogeneous precipitation of calcium phosphate (CaP) phases.

### 2.2 Culture of hMSCs

The hMSCs were purchased from Lonza (Walkersville, MD, USA) and were cultured in minimum essential culture medium (alpha-MEM) (Gibco, Invitrogen, Grand Island, NY, USA) supplemented with 10% fetal bovine serum and 1% penicillin/ streptomycin at 37°C in a 5% carbon dioxide ($CO_2$) incubator. The hMSCs between passages 5 and 8 were used for all experiments with seeding density of $1 \times 10^6$ cells/ml.

### 2.3 2-Hydroxyethyl agarose network synthesis

2-Hydroxyethyl agarose powder was added to alpha-MEM to yield a 4% w/v solution and autoclaved for 30 min. Solutions were then pipetted into cylindrical silicon rubber moulds (~5 mm diameter, ~2 mm height), pressed between glass plates, and cooled at 4°C for at least 10 min. Gels were then placed in alpha-MEM to equilibrate for at least 24 h before use.

### 2.4 Acellular IPN formation

A 20% w/v solution of PEG-DA (MW 6000 Da) in alpha-MEM was prepared, and 5 μl of Irgacure 651 photoinitiator solution (0·05% w/v in deionised (DI) water) was added to each millilitre of PEG-DA solution. Four cylindrical 2-hydroxyethyl agarose gels were added per millilitre of PEG-DA/photoinitiator solution and soaked under constant agitation at room temperature. The length of soaking time needed for adequate diffusion was calculated based on data from the literature[38] and was dependent on the PEG-DA MW. The 2-hydroxyethyl agarose gels were then placed in rectangular moulds (~2 mm height) between two optical glass microscope slides, and the surrounding volume was filled with excess PEG-DA/alpha-MEM soaking solution. The gels were exposed to ultraviolet (UV) light 2 min on each side using 365 nm light (9 mW/cm², Uvitec, Cambridge, UK). Samples were then cut using a 3 mm biopsy punch and added to phosphate-buffered saline (PBS) to equilibrate for at least 24 h before use. The formulations are reported according to the following structure: 2-hydroxyethyl agarose concentration/PEG-DA concentration (PEG-DA MW). As an example, the formulation 4-20 IPN is

an IPN with 4% w/v 2-hydroxyethyl agarose soaked in a 20% w/v PEG-DA (6000 Da MW) monomer solution prior to photopolymerisation.

### 2.5 Fabrication of nHAp-coated-PLGA microspheres

PLGA microspheres were fabricated using a water-in-oil-in-water ($W_1/O/W_2$) double-emulsion method. Briefly, 100 μl of double distilled water was poured into a 1 ml solution of PLGA in ethyl acetate (Fisher Scientific) with 5% w/v concentration. The mixture was mixed using a probe sonicator at 40 W power output for 15 s to form the first inner water-in-oil emulsion ($W_1/O$). This $W_1/O$ emulsion was poured into 1 ml of 5% polyvinyl alcohol (PVA) saturated with ethyl acetate and mixed using a vortex mixer for 15 s to form a second $W_1/O/W_2$ emulsion. The resulting $W_1/O/W_2$ double emulsion was poured into 200 ml of 0·3% PVA and continuously stirred at room temperature for 3 h until most of the ethyl acetate evaporated, leaving solid microspheres. The microspheres were collected using 0·22 μm Steritop filter (Millipore Corp., Billerica, MA, USA) and transferred to a 50 ml conical tube using a minimum amount of DI water. The microspheres were collected as a pellet by spinning in an ALC PK121 centrifuge (ALC International, Italy) at 4000 revolutions per minute (rpm) for 10 min. The microspheres were washed with double-distilled water twice. After washing, the microspheres were hydrolysed for 10 min in 0·5 M sodium hydroxide (NaOH) to functionalise the polymer surface and were rinsed in distilled water. The microspheres were immediately placed in mSBF (pH = 6·8), incubated at 37°C for 7 d, making sure to change the solution daily to maintain appropriate ion concentrations, frozen overnight at −80°C and lyophilised for 3 d. Both non-mineralised and mineralised microspheres were strained through a testing sieve to collect particles with a diameter of less than 250 μm to avoid microsphere clumping. The microspheres were sterilised under UV light for 16–18 h prior to use.

### 2.6 nHAp-coated microspheres and hMSC encapsulation in IPN network

A solution of 5% w/v 2-hydroxyethyl agarose in alpha-MEM was prepared and autoclaved for 30 min. Meanwhile, cells were detached from their flasks with trypsin-ethylenediaminetetraacetic acid and labelled as passage 1 (P1). At this point, P1 cells were pooled and resuspended in PBS at $1 \times 10^6$ cells/ml to begin the encapsulation procedure. Once cooled to 39°C, the cell suspension was added to a solution of molten 2-hydroxyethyl agarose in a 1:2 ratio to produce a 4% 2-hydroxyethyl agarose solution with a seeding density of $1 \times 10^6$ cells/ml (hMSCs) along with nHAp-coated PLGA microspheres (10 mg/ml). Each solution was pipetted into sterilised silicon rubber moulds (~5 mm diameter, ~2 mm height), pressed between two glass plates, and cooled at 4°C for 10 min. The cell-encapsulated gels were then added to the wells of an untreated 24-well plate in 1·5 ml growth medium (alpha-MEM) and incubated at 37°C/5% carbon dioxide. After 24 h, the gels were added to sterile filtered solutions of 20% w/v PEG-DA (6000 Da MW) with 0·05% w/v Irgacure 651 photoinitiator in alpha-MEM growth medium. Cell and nHAp-

**Bioinspired, Biomimetic and Nanobiomaterials**
Volume 5 Issue BBN1

**Biomineralised interpenetrating network hydrogels for bone tissue engineering**
Ingavle, Avadhanam, Zheng, Liu and Sandeman

coated microsphere-encapsulated 2-hydroxyethyl agarose gels were incubated at 37°C for 6 h with constant agitation for diffusion times dependent on the MW of PEG-DA. Afterwards, the gels were placed in sterilised rectangular silicon moulds (filled with excess PEG-DA/alpha-MEM soaking solution) between sterilised optical glass microscope slides and exposed for 2 min on each side to 365 nm light (9 mW/cm$^2$). The gel samples were then cut using a 3 mm biopsy punch and returned to growth media for 24 h before analysis.

### 2.7 Swelling degree measurement

Acellular IPN gels were placed in excess DI water for at least 24 h to remove extractable materials from the polymer networks. Equilibrated cell-free gel samples were weighed and dried in a lyophiliser. After at least 48 h, the dried gel samples were removed and weighed again. The swelling degree $Q$ was calculated as the ratio of the weight of the equilibrated hydrogel sample to its dry weight.

### 2.8 Mechanical testing

The compressive modulus of the IPN hydrogels was determined at room temperature on a TA.XTplus texture analyser (from Stable Micro Systems) and tested under unconfined uniaxial compression with a 5 N load cell ($n = 5$). All measurements and mechanical testing were performed on IPN gels swollen to equilibrium in alpha-MEM, and compression plates were lubricated with mineral oil both to minimise any gel–plate adhesion and to prevent gel drying during testing. Following a tare load of 5 N, the hydrogels were then compressed in the direction normal to the circular face of the IPN gel at a rate of 0·05 mm/s (1·7%/min) until fracture occurred. The compressive elastic modulus, defined as the slope of the linear region of the stress–strain curve of a material under compression, was calculated from the initial linear portion of the curve (<20% strain). Fracture points were identified at the peak stress after which a significant (>10%) decrease in stress occurred. The compressive moduli were calculated using the neo-Hookean model for ideal elastomers. For this model, a plot of stress against the strain function $\lambda - 1/\lambda^2$ yields a straight line up to a strain $\varepsilon$ of 0·5 or greater, where $\lambda = L/L_0 = 1 + \varepsilon$.[39] The compressive moduli were reported as mean values from sets of at least five samples.

### 2.9 Scanning electron microscopy and transmission electron microscopy analysis

For scanning electron microscopy (SEM) imaging, the fully hydrated IPN samples were sectioned to a thickness of 1 mm. To avoid ice formation altering the existing IPN internal structure, low-temperature instant freezing was employed to encourage the formation of smaller ice crystals prior to the freeze-drying process. Sections of IPN samples were frozen at −80°C before being transferred to a Christ freeze-dryer to remove the water from the IPN matrix over night at 0·200 mbar vacuum pressures. The freeze-dried IPN slices were mounted on a sample holder and coated with a 4-nm-thick layer of platinum using a Quorum (Q150T ES) coater. The sections were examined using a Zeiss Sigma field-emission

gun SEM (Zeiss NTS) at an accelerating voltage of 5 kV at different magnifications. The nanocoating of HAp on PLGA surface was investigated by high-resolution transmission electron microscopy (TEM) on a JEM-2100 microscope (Jeol, Tokyo, Japan). For TEM observation, nHAp-coated PLGA microspheres were suspended in ethanol and sprayed over a copper (Cu) TEM grid with a holey carbon (C) film before TEM imaging.

### 2.10 Live/dead assay

To compare the viability of cells cultured in the IPN with and without nHAp-coated microspheres, a live/dead assay was performed immediately after 24 h, 48 h and 1 week of culture ($n = 3$) using a live/dead viability cytotoxicity kit (Molecular Probes). This kit contains 2 mM calcein AM to stain the living cells and 4 mM ethidium homodimer-1 to stain the dead cells. Cylindrical hydrogel constructs ($n = 3$) were sectioned horizontally into two equal halves and incubated in the Live/Dead reagents for 30 min before imaging to promote thorough staining. Fluorescence spinning-disc confocal microscopy was used to visualise the green living cells and the red dead cells, using a Zeiss LSM-410 confocal microscope with 488 nm excitation/515–540 nm emission and 561 nm excitation/585 long-pass emission filters with a charge-coupled device camera. Z scans were performed to 350–500 μm resolution depth in areas representative of the overall IPN gels. Images were acquired in 2 × 2 binning mode. The three-dimensional (3D) images were deconvoluted using a constrained iterative algorithm (SlideBook). The percentage of total viable cells was calculated using the SlideBook (version 5.0) Mask Statistics module.

### 2.11 Osteogenic response in cell culture

The 4-20 IPN and composite 4-20 IPN + nHAp gel samples ($n = 4$ per group) were subsequently rinsed with PBS (Sigma) and collected in 400 μl of passive lysis buffer (Promega, Madison, WI, USA). Immediately following one freeze–thaw cycle, lysates were sonicated briefly and centrifuged for 5 min at 10 000 rpm, and the supernatant was used to determine deoxyribonucleic acid (DNA) content, calcium content and intracellular alkaline phosphatase (ALP) activity. The total DNA present in each hydrogel construct was quantified using the Quant-iT PicoGreen double-stranded DNA kit (Invitrogen) in comparison to a known standard curve. Intracellular ALP from hMSC-seeded IPN scaffolds was quantified using a $p$-nitrophenyl phosphate colorimetric assay at 405 nm as described.[25] The ALP activity was normalised to DNA content determined as described above. The total calcium present on hMSC-seeded IPN hydrogel scaffolds was measured using an $o$-cresolphthalein complexon colorimetric assay similar to that previously described.[25] Briefly, minced hydrogel discs were incubated in 0·9 N sulfuric acid ($H_2SO_4$) overnight to solubilise surface calcium deposits. The calcium concentration in solution was then quantified and compared with a known standard curve. To account for the calcium present in the nHAp-coated PLGA microsphere-loaded IPN samples, the calcium in acellular IPN gels was quantified at each time point and subtracted from the calcium values obtained from IPN gels containing cells at each time point.

**Bioinspired, Biomimetic and Nanobiomaterials**
Volume 5 Issue BBN1

**Biomineralised interpenetrating network hydrogels for bone tissue engineering**
Ingavle, Avadhanam, Zheng, Liu and Sandeman

## 2.12 Statistical analysis

Statistical analysis was performed using two-way analysis of variance with the Bonferroni post-test, applying the correction for multiple comparisons at a significance level of $p < 0.05$ with Graph-Pad Prism 5 for Windows (GraphPad Software, La Jolla, CA, USA).

## 3. Results and discussion

In recent years, tailor-made hydrogels have demonstrated their capacity to guide tissue growth by biomolecular interactions with cells or adjacent tissues, in order to fine-tune their basic functions.[40] Still, several disadvantages of traditionally synthesised hydrogels particularly with regard to the loss of mechanical properties over time make their use for hard tissue applications often unsatisfactory.[41] Designing tissue-engineered scaffolds for bone tissue regeneration with the essential mechanical properties and favourable HA-rich micro-environment to promote cell attachment, growth and new tissue formation is one of the key challenges facing the bone tissue-engineering field. Previously, the authors investigated 2-hydroxyethyl agarose-PEG-based (IPN hydrogels that exhibited cytocompatibility and improved mechanical properties relative to its component networks).[12] The current study focused on further improving the mechanical properties of these composite IPNs by incorporating nHAp and investigating ECM mimetic bone-like micro-environments, essential for promoting cell growth and biosynthesis in IPNs.

## 3.1 nHAp-coated PLGA microspheres

nHAp-coated polymer microspheres were prepared here by way of a two-step process involving (*a*) formation of biodegradable PLGA microspheres using a standard water-in-oil-in-water (W/O/W) double-emulsion process[42] and (*b*) coating of PLGA microspheres with an inorganic nHAp by way of incubation in an mSBF, an aqueous solution that contains the ionic constituents of blood plasma with two-fold higher concentrations of calcium and phosphate ions[43] (Figure 1). The presence of Ca and phosphorus (P) peaks, along with carbon and oxygen (O) peaks associated with the PLGA polymer, were confirmed by energy-dispersive X-ray spectroscopy (EDX) (Figure 2(a)). The average calcium/phosphorus ratio is 2·3, which is within the range of biological apatites.[44] SEM (Figure 2(b)) and TEM images (Figures 2(c) and 2(d)) indicate that the nHAp mineral film is continuous on the microsphere surface and has a plate-like nanostructure. Therefore, the nHAp mineral layer grown on biodegradable polymer microspheres is similar in composition and morphology to bone mineral. In addition, the nHAp-coated PLGA microspheres have shown a rougher surface. It has been shown that this rough surface stimulates osteoblastic cell adhesion, growth and proliferation[45] and provides good biological fixation to the surrounding tissue.[46] Besides the carboxyl group of the PLGA microsphere, there are two other main factors that can affect nHAp growth: the concentration of calcium and phosphorus in the solution and the incubation time. Since mSBF contains
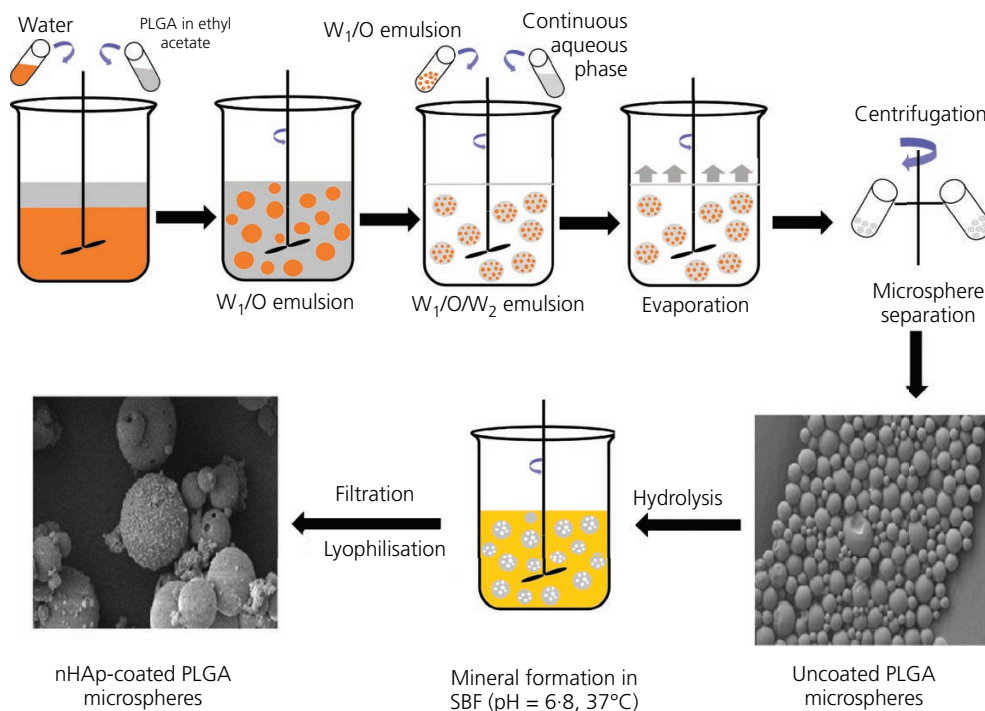


**Figure 1.** Schematic illustration of the formation of PLGA microspheres by the double-emulsion method and nHAp coating on microsphere surface. Mineralisation was carried out on hydrolysed PLGA microspheres using an mSBF for 5–7 d at 37°C, and the solutions were changed daily in order to replenish the ion concentration to supersaturated levels. SEM images show uncoated and mineral-coated microspheres after incubation in mSBF solutions

**Bioinspired, Biomimetic and Nanobiomaterials**
Volume 5 Issue BBN1

**Biomineralised interpenetrating network
hydrogels for bone tissue engineering**
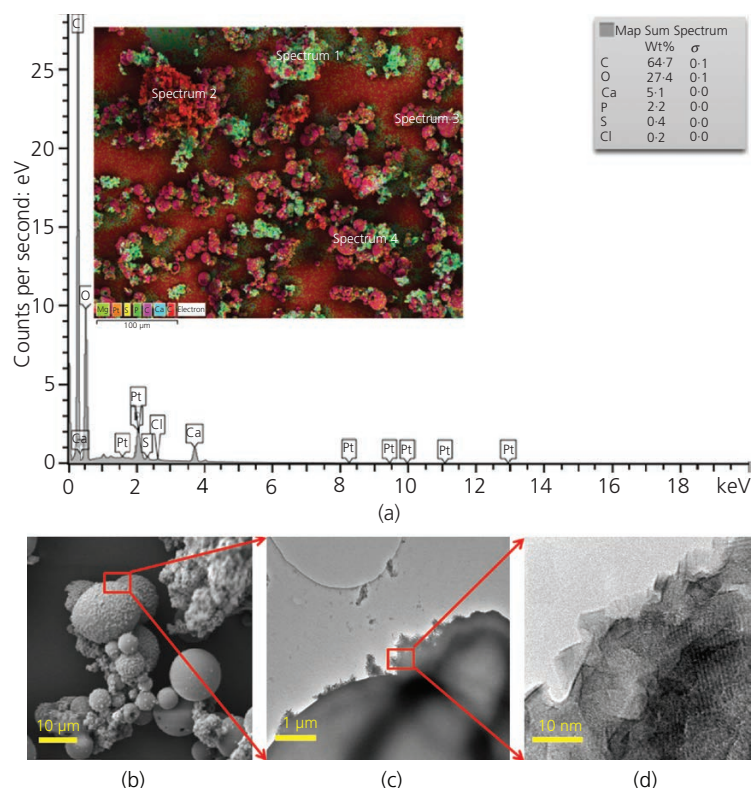Ingavle, Avadhanam, Zheng, Liu and Sandeman

**Figure 2.** SEM and TEM analysis results showing the calcium phosphate agglomerates are HAp crystals. (a) EDX scan spectra of nHAp-coated PLGA microspheres; inset shows the weight percentages and quantitative results of EDX spectrum of nanohydroxyapatite. (b) SEM micrograph showing continuous coating of nHAp mineral on microsphere surface. (c, d) TEM images showing the crystal structures of the nanoscale nHAp-coating layers

magnesium (II) ($Mg^{2+}$), sodium ($Na^+$) or carbonate ($CO_3^{2-}$) ions, which can also affect the nucleation and growth of nHAp coating, 6–7 d are needed at 37°C (pH = 6·8) to precipitate nHAp coating on the microspheres.

## 3.2 Physical and mechanical properties of composite nHAp/IPN hydrogel

The IPN gels were synthesised by way of a two-step network formation: the first step was the formation of a rigid, brittle 2-hydroxyethyl agarose gel network and the second was the formation of a softer and more ductile PEG-DA (20% w/v, MW = 6000) network within the first network by way of UV photo-cross-linking (Figure 3). In a previous study, Dekosky et al.[12] introduced a rationally designed 2-hydroxyethyl agarose/PEG-DA IPN hydrogel that exhibited dramatically improved mechanical properties relative to its component networks while maintaining cell viability for cartilage tissue-engineering application. However, there was still an opportunity for improvement in both mechanical properties and cell performance, which the authors hypothesised could be achieved with the inclusion of biomineralised nHAp-coated PLGA microspheres within the IPN gel. Compression analysis was carried out to assess the mechanical properties using a mechanical texture analyser fitted with a 5 N load cell (Figure 4(a)). The representative stress–strain curves for the plain IPN and

nHAp-coated PLGA microsphere-loaded IPN hydrogel groups are displayed in Figure 4(b). The compressive moduli were calculated from the slope of the initial linear neo-Hookean region of the stress–strain (<20% strain) curves. The inclusion of biomineralised nHAp-coated PLGA microspheres showed improvement in the amount of stress the gels could withstand before failure (Figure 4(b)). The inclusion of nHAp-coated PLGA microspheres in the composite IPN hydrogel (4-20 IPN + nHAp) produced a 2·7-fold ($p < 0.05$) increase in compressive modulus relative to a plain IPN hydrogel (4-20 IPN) (7500 against 2800 Pa) (inset of Figure 4(b)).

Swelling degree is an important parameter of hydrogel networks since it determines whether the IPN hydrogels provide a micro-environment favourable to waste/nutrient transport. The swelling degree is a key property for the hydrogels, because not only does it affect the mechanical properties of the material but also it impacts solute transport, influences cell behaviour and thus overall cell viability. Thus, the swelling degrees of acellular gels with and without nHAp were characterised. Macroscopic images of gels are displayed in Figure 5(a). The swelling degrees of equilibrium-swollen plain 4-20 IPN and 4-20 IPN hydrogel with encapsulated nHAp-coated PLGA microspheres are shown in Figure 5(b). The inclusion of nHAp-coated PLGA microspheres

**Bioinspired, Biomimetic and Nanobiomaterials**
Volume 5 Issue BBN1

**Biomineralised interpenetrating network
hydrogels for bone tissue engineering**
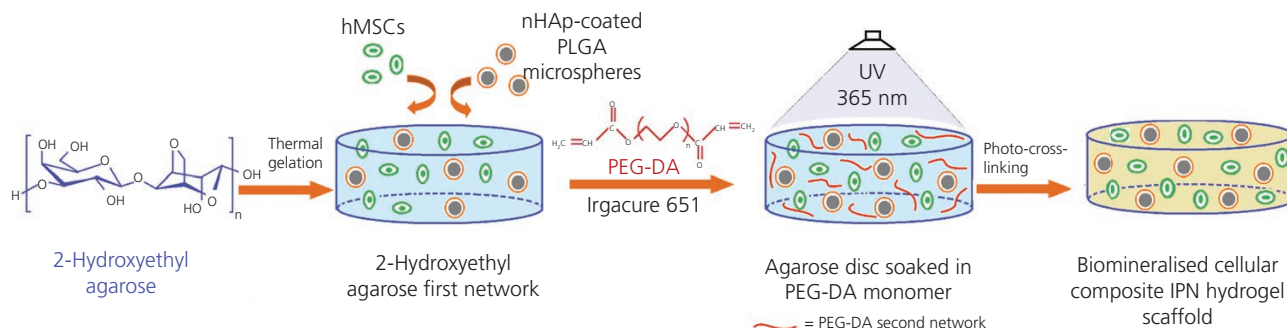Ingavle, Avadhanam, Zheng, Liu and Sandeman

**Figure 3.** Schematic representation showing the formation of cellular composite 2-hydroxyethyl agarose/PEG-DA IPNs containing nHAp-coated PLGA microspheres. To introduce nHAp, a naturally occurring mineral (main mineral component of bone), into the IPN, nHAp-coated PLGA microspheres were incorporated during synthesis of 2-hydroxyethyl agarose first network
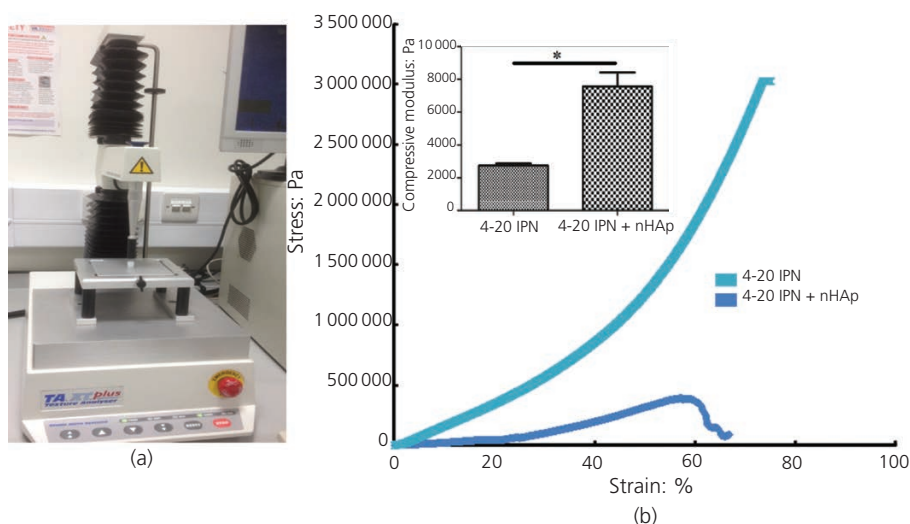


**Figure 4.** (a) Compression testing analyser and (b) representative stress-against-strain curves of IPN hydrogels with and without nHAp-coated PLGA microspheres. The samples ($n = 5$) were placed between force plates and compressed at a constant rate of 0·05 mm/s

produced a 20% decrease in swelling degree compared to the plain IPN hydrogel, but this decrease in swelling degree was not statistically significant.

The hMSCs and nHAp-coated PLGA microspheres are entrapped homogeneously inside the Ag/PEG-DA IPN gels during the gelation process aseptically in order to create 3D cell-seeded constructs. Microscopic image analysis revealed a uniform distribution of nHAp-coated PLGA microspheres and hMSCs inside the 2-mm-thick composite IPN hydrogels (Figure 6). SEM images of the acellular composite IPN show the uniform distribution of embedded nHAp-coated PLGA microspheres at the surface of (Figure 6(a)) and inside (Figure 6(b)) the IPN hydrogel. The beaded morphology of the nHAp-coated PLGA microspheres in the cross-sectional SEM images (Figure 6(b))

suggests a uniform distribution and confirms the presence of a highly percolative and interconnected macroporous network with a highly ordered architecture and well-defined pore boundaries. The phase-contrast micrographs (Figure 6(c)) indicate that the encapsulated hMSCs were homogeneously distributed with a rounded morphology within the composite IPN gel, while live/dead (calcein AM-ethidium dye) cell staining indicated that the majority of cells encapsulated in the composite IPN hydrogels remained viable during the photo-polymerisation process upon UV exposure (Figure 6(d)).

### 3.3 Cell viability
A live/dead assay was used to determine cell viability at different time intervals after hMSC encapsulation (Figure 7). Comparison of cells at incubation days 1 and 21 using live/dead (calcein AM-

**Bioinspired, Biomimetic and Nanobiomaterials**
Volume 5 Issue BBN1

**Biomineralised interpenetrating network
hydrogels for bone tissue engineering**
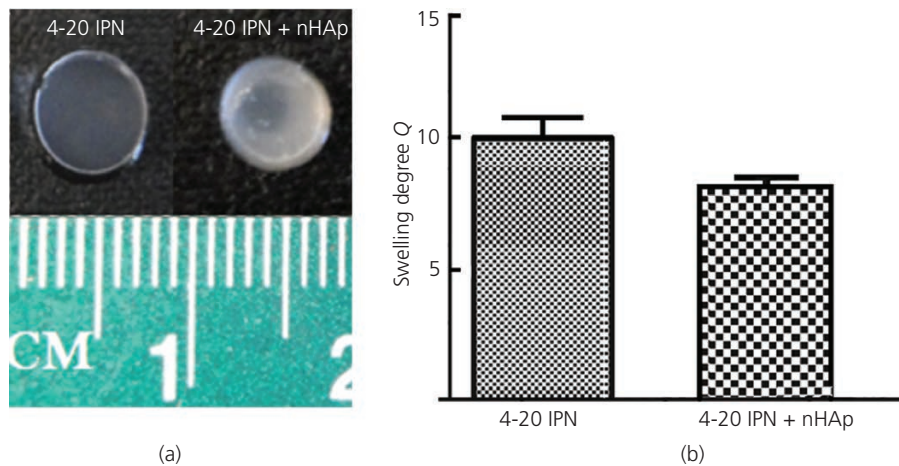Ingavle, Avadhanam, Zheng, Liu and Sandeman

(a)　　　　　(b)

**Figure 5.** (a) Representative macroscopic images and (b) swelling
degrees of equilibrium swelled IPN gels with and without
nHAp-coated PLGA microspheres. Note the reduction in transparency
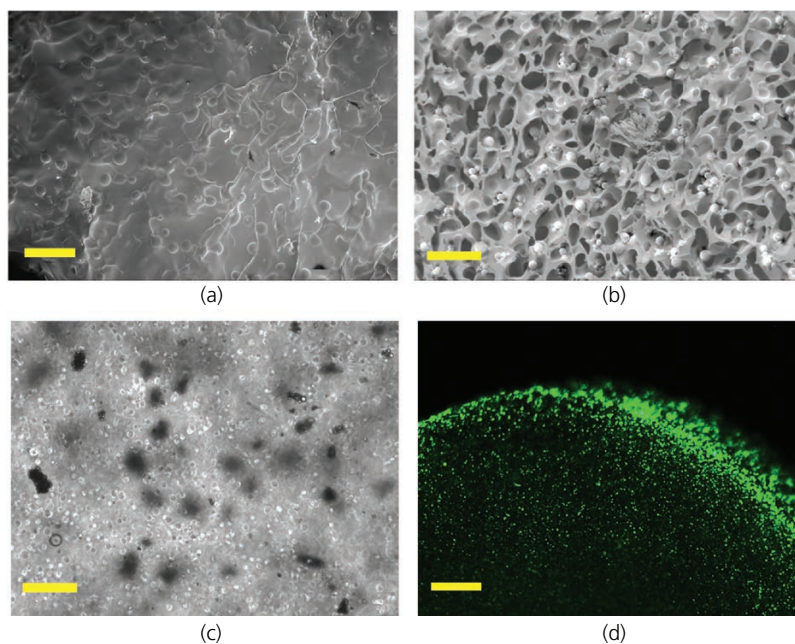with encapsulated mineral-coated microspheres



(a)　　　　　(b)

(c)　　　　　(d)

**Figure 6.** Representative SEM micrographs showing (a) surface and
(b) internal morphologies of acellular IPN gel with uniformly
distributed nHAp-coated PLGA microspheres (scale bar = 100 μm).
(c) Phase-contrast photomicrograph of encapsulated hMSCs along with
nHAp-coated microspheres. The dotted spots indicate encapsulated
PLGA microspheres (scale bar = 200 μm). (d) Confocal laser scanning
fluorescence microscope image of composite IPN hydrogel, showing
live (green fluorescence) hMSCs at day 1 (scale bar = 300 μm)

ethidium dye) cell staining indicated that the majority of cells
encapsulated in composite hydrogels containing nHAp-coated
PLGA microspheres remained viable (stained fluorescent green
with calcein AM) over the culture period of 3 weeks (Figure 7).
The viability of hMSCs in nHAp-coated PLGA microsphere-free
IPN hydrogels was high, but less than optimal. At day 21, the cell
viability in 4-20 IPN+ nHAp hydrogel was higher than that in

the plain 4-20 IPN hydrogel by a factor of 1·4 ($p < 0·05$).
An additional observation was that encapsulated hMSCs in nHAp-
free IPN gel were homogeneously distributed and isolated from
each other (Figure 7(b)) compared with the hMSCs encapsulated
in the presence of nHAp-coated PLGA microspheres, which
appeared as clusters (Figure 7(d)). This indicated that good
adhesion and proliferation of hMSCs on the surface of PLGA

**Bioinspired, Biomimetic and Nanobiomaterials**
Volume 5 Issue BBN1

**Biomineralised interpenetrating network hydrogels for bone tissue engineering**
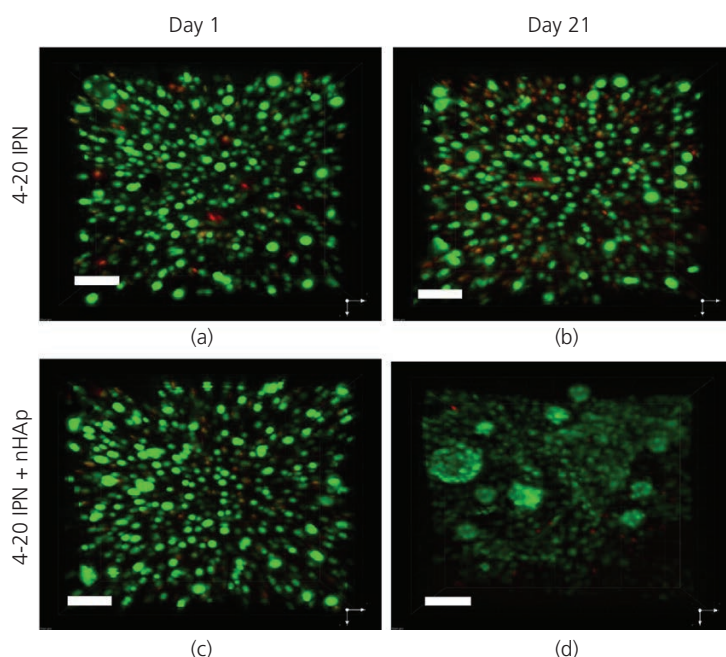Ingavle, Avadhanam, Zheng, Liu and Sandeman

**Figure 7.** 3D projections of spinning disc confocal microscope showing live/dead images for plain IPN and composite IPN groups. (a, b) Plain 4-20 IPN gels with encapsulated hMSCs at days 1 and 21 respectively. (c, d) Composite 4-20 IPN + nHAp gels with encapsulated hMSCs at days 1 and 21 respectively. Green (calcein AM) dye indicates viable (live) cell populations, while red (ethidium homodimer) dye indicates dead cells. Scale bar = 100 μm

microspheres resulted in the formation of microsphere-cell clusters. Mask statistics analysis showed that in the absence of nHAp-coated PLGA microspheres (4-20 IPN), viability dropped significantly ($p < 0.05$) from 95·9% to 59·1% at 3 weeks post-encapsulation in culture respectively, while incorporating nHAp-coated PLGA microsphere within the IPN (4-20 IPN + nHAp) improved cell viability to 80·6% (Figure 8). The inclusion of mineralised nHAp-coated PLGA microspheres provided nucleation sites for calcium and phosphate secreted by entrapped hMSCs and improved cell viability.
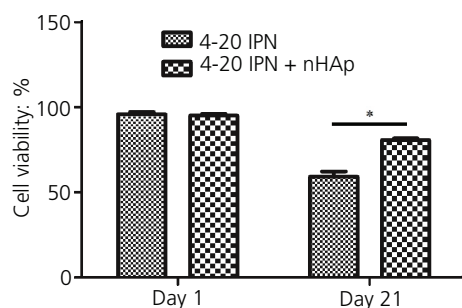


**Figure 8.** Cell viability percentage of encapsulated hMSCs by image analysis mask statistics. Multiple confocal Z-scan series were performed on a representative sample in each group (mean ± standard deviation (SD)). The * indicates statistically significant differences ($p < 0.05$ and $n = 3$)

### 3.4 Osteogenic response in cell culture

Production and accumulation of major bone components such as ALP and calcium were measured (Figure 9). ALP activity is an important marker of early osteogenic differentiation. The ALP activity within hMSC-seeded 4-20 IPN and 4-20 IPN + nHAp gel scaffolds displayed significant differences (Figure 9(a)). A time-dependent increase in ALP activity was observed in all gel groups from day 1 to day 21. There were no statistically significant differences in ALP expression among groups at day 1. At day 14, there was a significant difference in ALP activity within the plain IPN and nHAp-coated microsphere-incorporated IPN hydrogel groups. ALP expression in the composite 4-20 IPN + nHAp gel was 1·6 times higher than that in the plain 4-20 IPN gel. At day 21, the ALP activity in the composite 4-20 IPN + nHAp gel was 2·6 times higher than in the plain 4-20 IPN gel. At days 14 and 21, the composite 4-20 IPN + nHAp gel group showed a 2·7- and 4·6-fold increase in ALP activity respectively relative to their values at day 1 ($p < 0.05$, $n = 3$). The higher values of ALP activity indicated enhanced early osteogenic differentiation of hMSCs cultured in the composite IPN hydrogel.

Calcium content was measured to assess the extent of matrix mineralisation in the IPN hydrogel scaffolds (Figure 9(b)). Calcium deposition or mineralisation occurs during the late stage of osteogenesis and is considered a marker of full osteogenic differentiation. Total calcium deposition from osteogenically induced hMSCs cultured in the plain 4-20 IPN and composite 4-20 IPN + nHAp gels was quantified after days 1, 14 and 21

**Bioinspired, Biomimetic and Nanobiomaterials**
Volume 5 Issue BBN1

**Biomineralised interpenetrating network hydrogels for bone tissue engineering**
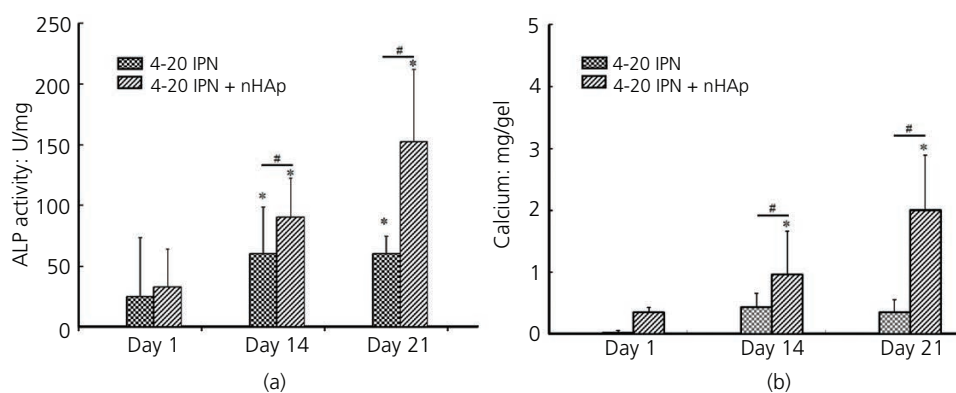Ingavle, Avadhanam, Zheng, Liu and Sandeman

**Figure 9.** Quantification of (a) ALP activity and (b) total calcium deposition on hMSC-seeded plain IPN and composite IPN hydrogels at days 1, 14 and 21. Chart values represent mean ± SD. Values with * indicate statistically significant increase against day 1, while values with # indicate statistically significant differences among the groups at that time point ($p < 0.05$, $n = 4$)

(Figure 9(b)). There was no statistically significant difference in total calcium deposition content among groups at day 1. At day 14, the total calcium deposition in the composite 4-20 IPN + nHAp gel group was 2·2 times higher than in the plain 4-20 IPN gel group, which in turn showed a threefold increase ($p < 0.05$) in total calcium deposition relative to values at day 1. Similarly, at day 21, the composite 4-20 IPN + nHAp gel alone also resulted in significantly greater ($p < 0.05$) calcium deposition by a factor of 6·6 than in the plain 4-20 IPN gel group. A composite 4-20 IPN + nHAp gel deposited almost tenfold higher calcium relative to its value at day 1 ($p < 0.05$). In contrast, at days 14 and 21 the plain 4-20 IPN gel group showed no significant difference in calcium deposition values relative to day 1.

## 4.    Conclusions

Double-network hydrogels have traditionally been restricted to soft tissue engineering because of their poor mechanical stability. The current study aimed to incorporate nHAp (bone-like mineral)-coated polymeric microspheres into IPN hydrogel scaffolds in order to improve the scaffolds' properties for hard tissue-engineering applications. A three-component IPN hydrogel composite was optimised, combining 2-hydroxyethyl agarose/PEG-DA, nHAp-coated PLGA microspheres and cells for augmented mechanical strength and cell support. By combining the polymer characteristics of 2-hydroxyethyl agarose/PEG-DA IPN hydrogels with those of HAp nanoparticles, elastomeric composite IPN hydrogels were synthesised with unique mechanical properties related to compressibility and toughness. This approach demonstrated the optimal number of nHAp-coated PLGA microsphere nanoparticles (10 mg/ml) to achieve significantly improved composite IPN hydrogel strength and bioactivity. In addition, the current method produced for the first time a homogeneous structure with superior stiffness in which a hydrated IPN matrix was highly mineralised and allowed cells to continuously proliferate. The addition of nHAp-coated PLGA microspheres provided cell adhesion sites for cell attachment to the PLGA microsphere surface and showed cell clustering around HAp-rich areas within the IPN matrix. The enhancement in the mechanical strength and the 3D deposition of bone apatite in the cell-laden composite indicates a new strategy by which IPN hydrogel-based supports may be augmented to direct bone tissue replacement and regeneration.

## Acknowledgements

**REFERENCES**

1. Cushing MC and Anseth KS (2007) Materials science: hydrogel cell cultures. *Science* **316(5828)**: 1133–1134.
2. Lee KY and Mooney DJ (2001) Hydrogels for tissue engineering. *Chemical Reviews* **101(7)**: 1869–1879.
3. Griffith LG and Swartz MA (2006) Capturing complex 3D tissue physiology in vitro. *Nature Reviews Molecular Cell Biology* **7(3)**: 211–224.
4. Calvert P (2009) Hydrogels for soft machines. *Advanced Materials* **21(7)**: 743–756.
5. Gong JP, Katsuyama Y, Kurokawa T and Osada Y (2003) Double-network hydrogels with extremely high mechanical strength. *Advanced Materials* **15(14)**: 1155–1158.
6. Huang M, Furukawa H, Tanaka Y *et al.* (2007) Importance of entanglement between first and second components in high-strength double network gels. *Macromolecules* **40(18)**: 6658–6664.
7. Kaneko D, Tada T, Kurokawa T, Gong JP and Osada Y (2005) Mechanically strong hydrogels with ultra-low frictional coefficients. *Advanced Materials* **17(5)**: 535–538.
8. Na YH, Kurokawa T, Katsuyama Y *et al.* (2004) Structural characteristics of double network gels with extremely high mechanical strength. *Macromolecules* **37(14)**: 5370–5374.

**Bioinspired, Biomimetic and Nanobiomaterials**
Volume 5 Issue BBN1

**Biomineralised interpenetrating network hydrogels for bone tissue engineering**
Ingavle, Avadhanam, Zheng, Liu and Sandeman

9. Nakayama A, Kakugo A, Gong JP *et al.* (2004) High mechanical strength double-network hydrogel with bacterial cellulose. *Advanced Functional Materials* **14(11)**: 1124–1128.

10. Yasuda K, Gong JP, Katsuyama Y *et al.* (2005) Biomechanical properties of high-toughness double network hydrogels. *Biomaterials* **26(21)**: 4468–4475.

11. Ingavle GC, Dormer NH, Gehrke SH and Detamore MS (2012) Using chondroitin sulfate to improve the viability and biosynthesis of chondrocytes encapsulated in interpenetrating network (IPN) hydrogels of agarose and poly(ethylene glycol) diacrylate. *Journal of Materials Science – Materials in Medicine* **23(1)**: 157–170.

12. DeKosky BJ, Dormer NH, Ingavle GC *et al.* (2010) Hierarchically designed agarose and poly(ethylene glycol) interpenetrating network hydrogels for cartilage tissue engineering. *Tissue Engineering Part C – Methods* **16(6)**: 1533–1542.

13. Ingavle GC, Gehrke SH and Detamore MS (2014) The bioactivity of agarose PEGDA interpenetrating network hydrogels with covalently immobilized RGD peptides and physically entrapped aggrecan. *Biomaterials* **35(11)**: 3558–3570.

14. Ingavle GC, Frei AW, Gehrke SH and Detamore MS (2013) Incorporation of aggrecan in interpenetrating network hydrogels to improve cellular performance for cartilage tissue engineering. *Tissue Engineering Part A* **19(11–12)**: 1349–1359.

15. Song J, Xu J, Filion T *et al.* (2009) Elastomeric high-mineral content hydrogel-hydroxyapatite composites for orthopedic applications. *Journal of Biomedical Materials Research Part A* **89(4)**: 1098–1107.

16. Hoppe A, Guldal NS and Boccaccini AR (2011) A review of the biological response to ionic dissolution products from bioactive glasses and glass-ceramics. *Biomaterials* **32(11)**: 2757–2774.

17. Zhou H and Lee J (2011) Nanoscale hydroxyapatite particles for bone tissue engineering. *Acta Biomaterialia* **7(7)**: 2769–2781.

18. Chang BS, Lee CK, Hong KS *et al.* (2000) Osteoconduction at porous hydroxyapatite with various pore configurations. *Biomaterials* **21(12)**: 1291–1298.

19. Kokubo T and Takadama H (2006) How useful is SBF in predicting in vivo bone bioactivity? *Biomaterials* **27(15)**: 2907–2915.

20. Murphy WL, Hsiong S, Richardson TP, Simmons CA and Mooney DJ (2005) Effects of a bone-like mineral film on phenotype of adult human mesenchymal stem cells in vitro. *Biomaterials* **26(3)**: 303–310.

21. Murphy WL and Mooney DJ (2002) Bioinspired growth of crystalline carbonate apatite on biodegradable polymer substrata. *Journal of the American Chemical Society* **124(9)**: 1910–1917.

22. Jongpoiboonkit L, Franklin-Ford T and Murphy WL (2009) Mineral-coated polymer microspheres for controlled protein binding and release. *Advanced Materials* **21(19)**: 1960–1963.

23. Kang SW, Yang HS, Seo SW, Han DK and Kim BS (2008) Apatite-coated poly(lactic-co-glycolic acid) microspheres as an injectable scaffold for bone tissue engineering. *Journal of Biomedical Materials Research Part A* **85A(3)**: 747–756.

24. Murphy WL, Simmons CA, Kaigler D and Mooney DJ (2004) Bone regeneration via a mineral substrate and induced angiogenesis. *Journal of Dental Research* **83(3)**: 204–210.

25. Davis HE, Binder BYK, Schaecher P *et al.* (2013) Enhancing osteoconductivity of fibrin gels with apatite-coated polymer microspheres. *Tissue Engineering Part A* **19(15–16)**: 1773–1782.

26. Gaharwar AK, Dammu SA, Canter JM, Wu CJ and Schmidt G (2011) Highly extensible, tough, and elastomeric nanocomposite hydrogels from poly(ethylene glycol) and hydroxyapatite nanoparticles. *Biomacromolecules* **12(5)**: 1641–1650.

27. Gaharwar AK, Rivera CP, Wu CJ and Schmidt G (2011) Transparent, elastomeric and tough hydrogels from poly (ethylene glycol) and silicate nanoparticles. *Acta Biomaterialia* **7(12)**: 4139–4148.

28. Gaharwar AK, Mihaila SM, Swami A *et al.* (2013) Bioactive silicate nanoplatelets for osteogenic differentiation of human mesenchymal stem cells. *Advanced Materials* **25(24)**: 3329–3336.

29. Gaharwar AK, Rivera C, Wu CJ, Chan BK and Schmidt G (2013) Photocrosslinked nanocomposite hydrogels from PEG and silica nanospheres: structural, mechanical and cell adhesion characteristics. *Materials Science & Engineering C – Materials for Biological Applications* **33(3)**: 1800–1807.

30. Gaharwar AK, Schexnailder P, Kaul V *et al.* (2010) Highly extensible bio-nanocomposite films with direction-dependent properties. *Advanced Functional Materials* **20(3)**: 429–436.

31. Gaharwar AK, Kishore V, Rivera C *et al.* (2012) Physically crosslinked nanocomposites from silicate-crosslinked PEO: mechanical properties and osteogenic differentiation of human mesenchymal stem cells. *Macromolecular Bioscience* **12(6)**: 779–793.

32. Dawson JI and Oreffo ROC (2013) Clay New opportunities for tissue regeneration and biomaterial design. *Advanced Materials* **25(30)**: 4069–4086.

33. Zhao L, Weir MD and Xu HH (2010) An injectable calcium phosphate-alginate hydrogel-umbilical cord mesenchymal stem cell paste for bone tissue engineering. *Biomaterials* **31(25)**: 6502–6510.

34. Gkioni K, Leeuwenburgh SC, Douglas TE, Mikos AG and Jansen JA (2010) Mineralization of hydrogels for bone regeneration. *Tissue Engineering Part B Reviews* **16(6)**: 577–585.

35. Hutchens SA, Benson RS, Evans BR, O'Neill HM and Rawn CJ (2006) Biomimetic synthesis of calcium-deficient hydroxyapatite in a natural hydrogel. *Biomaterials* **27(26)**: 4661–4670.

36. Sohier J, Corre P, Weiss P and Layrolle P (2010) Hydrogel/calcium phosphate composites require specific properties for three-dimensional culture of human bone mesenchymal cells. *Acta Biomaterialia* **6(8)**: 2932–2939.

**Bioinspired, Biomimetic and Nanobiomaterials**
Volume 5 Issue BBN1

**Biomineralised interpenetrating network hydrogels for bone tissue engineering**
Ingavle, Avadhanam, Zheng, Liu and Sandeman

37. Murphy WL, Kohn DH and Mooney DJ (2000) Growth of continuous bonelike mineral within porous poly(lactide-co-glycolide) scaffolds in vitro. *Journal of Biomedical Materials Research* **50(1)**: 50–58.

38. Weng LH, Liang SM, Zhang L, Zhang XM and Xu J (2005) Transport of glucose and poly(ethylene glycol)s in agarose gels studied by the refractive index method. *Macromolecules* **38(12)**: 5236–5242.

39. Treloar LRG (1975) *The Physics of Rubber Elasticity*. Clarendon Press, Oxford, UK.

40. Lutolf MP and Hubbell JA (2005) Synthetic biomaterials as instructive extracellular microenvironments for morphogenesis in tissue engineering. *Nature Biotechnology* **23(1)**: 47–55.

41. Kopecek J and Yang JY (2007) Review – hydrogels as smart biomaterials. *Polymer International* **56(9)**: 1078–1098.

42. Meng FT, Ma GH, Qiu W and Su ZG (2003) W/O/W double emulsion technique using ethyl acetate as organic solvent: effects of its diffusion rate on the characteristics of microparticles. *Journal of Controlled Release* **91(3)**: 407–416.

43. Murphy WL and Messersmith PB (2000) Compartmental control of mineral formation: adaptation of a biomineralization strategy for biomedical use. *Polyhedron* **19(3)**: 357–363.

44. Elliott JC (1994) *Structure and Chemistry of the Apatites and Other Calcium Orthophosphates*. Elsevier, New York, NY, USA.

45. Seyfoori A, Mirdamadi S, Mehrjoo M and Khavandi A (2013) In-vitro assessments of micro arc oxidized ceramic films on AZ31 magnesium implant: degradation and cell-surface response. *Progress in Natural Science-Materials International* **23(4)**: 425–433.

46. Li W, Guan SK, Chen J *et al.* (2011) Preparation and in vitro degradation of the composite coating with high adhesion strength on biodegradable Mg-Zn-Ca alloy. *Materials Characterization* **62(12)**: 1158–1165.